

Using Random Forest Model Combined With Gabor Feature to Predict Protein-Protein Interaction From Protein Sequence

Xin-Ke Zhan, Zhu-Hong You, Li-Ping Li, Yang Li, Zheng Wang and Jie Pan

School of Information Engineering, Xijing University, Xi'an, China.

Evolutionary Bioinformatics
Volume 16: 1–10
© The Author(s) 2020
Article reuse guidelines:
sagepub.com/journals-permissions
DOI: 10.1177/1176934320934498



ABSTRACT: Protein-protein interactions (PPIs) play a crucial role in the life cycles of living cells. Thus, it is important to understand the underlying mechanisms of PPIs. Although many high-throughput technologies have generated large amounts of PPI data in different organisms, the experiments for detecting PPIs are still costly and time-consuming. Therefore, novel computational methods are urgently needed for predicting PPIs. For this reason, developing a new computational method for predicting PPIs is drawing more and more attention. In this study, we proposed a novel computational method based on texture feature of protein sequence for predicting PPIs. Especially, the Gabor feature is used to extract texture feature and protein evolutionary information from Position-Specific Scoring Matrix, which is generated by Position-Specific Iterated Basic Local Alignment Search Tool. Then, random forest-based classifiers are used to infer the protein interactions. When performed on PPI data sets of yeast, human, and *Helicobacter pylori*, we obtained good results with average accuracies of 92.10%, 97.03%, and 86.45%, respectively. To better evaluate the proposed method, we compared Gabor feature, Discrete Cosine Transform, and Local Phase Quantization. Our results show that the proposed method is both feasible and stable and the Gabor feature descriptor is reliable in extracting protein sequence information. Furthermore, additional experiments have been conducted to predict PPIs of other 4 species data sets. The promising results indicate that our proposed method is both powerful and robust.

KEYWORDS: Protein sequence, protein-protein interactions, Gabor features, random forest

RECEIVED: March 05, 2020. **ACCEPTED:** May 20, 2020.

TYPE: Methods and Protocols

FUNDING: The author(s) disclosed receipt of the following financial support for the research, authorship, and/or publication of this article: This research is funded by the National Natural Science Foundation of China under Grant (No. 61722212 and 61873212.)

DECLARATION OF CONFLICTING INTERESTS: The author(s) declared no potential conflicts of interest with respect to the research, authorship, and/or publication of this article.

CORRESPONDING AUTHORS: Zhu-Hong You, School of Information Engineering, Xijing University, Xi'an 710123, China. Email: zhuhongyou@gmail.com

Li-Ping Li, School of Information Engineering, Xijing University, Xi'an 710123, China. Email: lipingli_szu@foxmail.com

Introduction

Proteins play significant roles in the life activities of cells and organisms, such as neurotransmission, DNA replication, and cycle control. Most of the diversity of cellular functions is based on protein-protein interactions (PPIs). Detecting PPIs is highly critical for the exploration of biological cellular mechanisms. With the advent of high-throughput techniques, such as mass spectrometric protein complex identification,¹ protein chip,² and yeast 2-hybrid system,^{3,4} considerable PPI data have been generated. However, high-throughput experiments are usually accompanied by high false positive and false negative rates and high cost. Moreover, these methods can hardly predict the whole PPI networks.⁵ Under this situation, developing a novel computational method to predict unknown PPIs is more urgent than adopting the traditional experimental method to identify PPI.^{6,7}

It is important to make full use of available PPI experimental data to develop computational methods. Many PPI databases, such as Human Protein References Database (HPRD),⁸ Database of Interacting Protein (DIP),⁹ and Molecular INteraction database (MINT),¹⁰ have been built after a number of experiments depicting PPI network. However, there are differences in protein structure information,^{11,12} protein domains, and so on. With new protein amino acid sequence data explosively growing, computational methods are urgently needed to detect the information of protein sequence.

In recent years, a number of computational methods have been proposed to extract the feature vectors mainly from the amino acid sequence.^{13–16} The discriminative feature can improve the performance of a classification model, and some computational methods were based on Chou's pseudo amino acid composition (PseAAC)^{17–19} that retains the information of protein sequence, although it only considers the influence of 3 kinds of characteristics. Furthermore, some new methods on feature vector extraction are based on kernels. The method proposed by Jaakkola et al²⁰ is the first to use Fisher kernel to detect homology. Shen et al²¹ proposed the support vector machine (SVM)-based method to predict PPIs. Leslie et al²² put forward the mismatch string kernel method, which detects protein amino acid sequence at a lower computational cost. The difference between a PseAAC-based method and a kernel-based method lies in the way of extracting the feature information, with the first extracting the feature directly from the protein sequence and the second retaining some prior information and extracting feature vectors more effectively.

In general, most of the computational methods use machine learning algorithms combining various descriptors of proteins. Concerning different kinds of protein data, the main existing computational approaches can be divided into 2 categories: one uses information from the structure of proteins and genomic context; the other uses information from protein



sequences. Moreover, newly discovered protein sequences grow exponentially in many different types of databases, and to shorten the gap between known protein sequence data and their interaction statuses, it is important to develop computational methods that directly use the information in protein sequences.

In this work, a novel computational method for predicting PPIs from an amino acid sequence based on a random forest (RF)²³ classification and a Gabor feature descriptor was proposed. The major improvement of this method is that it extracts protein sequence features through Gabor texture representation. Specifically, we adopted the Gabor feature representation on a Position-Specific Scoring Matrix (PSSM)^{24,25} to extract the evolutionary information from protein sequence, and then a classification RF is applied to infer the PPIs. In this way, each protein sequence is represented as a PSSM. To obtain more feature descriptors, we use a Gabor descriptor to extract features in each protein PSSM, and then each protein sequence is represented by 100-dimensional feature vectors. Two corresponding feature vectors would be joint together and represent a protein pair as a 200-dimensional feature vector. Finally, we used RF as a machine learning classifier for classification. The method was adopted for 3 PPI data sets from *human*, *yeast*, and *Helicobacter pylori*. Our results indicate that the computational method has good performance. To further evaluate the performance of this method, we compared the results of the proposed method with the support vector machine classifier to the Gabor feature, Discrete Cosine Transform (DCT),²⁶ and Local Phase Quantization (LPQ).²⁷ Moreover, we also used our approach for predicting the PPIs in 4 other species using the protein interaction data from *yeast*. The results of the proposed method in predicting PPIs indicate this approach is trustworthy.

Materials and Methods

Golden standard data sets

From the public DIP, we collected *Saccharomyces cerevisiae* PPI data sets. Then, the protein pairs that contain a protein with less than 50 residues or have more than 40% sequence identity were removed. The positive data set was constructed with the remaining 5594 protein pairs. The negative data set was constructed with the 5594 noninteracting protein pairs, which have different subcellular localization. Finally, we constructed 11 188 protein pairs, of which half are from the positive data set and half from the negative data set.

Two other PPI data sets were also collected. The first PPI data set was collected from the HPRD. The protein pairs with more than 25% sequence identity were removed. We constructed the golden standard positive data set with the remaining 3899 protein-protein pairs of experimentally verified PPIs from 2502 different human proteins. Following previous work,²⁸ we assumed that proteins in different subcellular compartments would not interact with each other. Therefore, 4262 protein pairs from 661 different human proteins were set as

the golden negative data set. The complete human data set consists of 8161 protein pairs. The other PPI data set was constructed with 2916 *H. pylori* protein pairs (1458 interacting pairs and 1458 noninteracting pairs), which were described by Martin et al.²⁹

Position-Specific Scoring Matrix

The PSSM is widely used in various biological research works, such as studies of subcellular localization, disordered regions, and protein secondary structure. The PSSM also has great potential in extracting evolutionary information from amino acid sequences. In this work, each protein sequence would be converted into PSSM by adopting a Position-Specific Iterated Basic Local Alignment Search Tool (PSI-BLAST).²⁴ The PSSM can be represented as follows:

$$\text{PSSM} = \begin{bmatrix} P_{1,1} & P_{1,2} & \cdots & P_{1,j} & \cdots & P_{1,20} \\ P_{2,1} & P_{2,2} & \cdots & P_{2,j} & \cdots & P_{2,20} \\ \vdots & \vdots & \vdots & \vdots & \vdots & \vdots \\ P_{i,1} & P_{i,2} & \cdots & P_{i,j} & \cdots & P_{i,20} \\ \vdots & \vdots & \vdots & \vdots & \vdots & \vdots \\ P_{L,1} & P_{L,2} & \cdots & P_{L,j} & \cdots & P_{L,20} \end{bmatrix} \quad (1)$$

where L is the length of an amino acid sequence and $P_{i,j}$ denotes the possibility that the i th amino acid of the given protein sequence mutates to amino acid j in the evolution process. To obtain highly homologous sequences, the parameters of PSI-BLAST (E -values) are set as 0.001 and 3 iterations are selected.

Gabor filter-based feature

First proposed by Gabor,³⁰ the Gabor filter is very similar to the visual stimulus response of cells in the human visual system. It has good characteristics in extracting local spatial and frequency domain information of targets. The Gabor feature is usually obtained by a convoluting image with a Gabor filter. Moreover, they have strong anti-interference ability in terms of image noise and illumination changes, and the most important advantages of Gabor filters are their translation, invariance to rotation, and scale. In image processing, the feature based on the Gabor filter is directly extracted from gray-level images. The 2-dimensional Gabor filter, in the spatial domain, is a Gaussian kernel function modulated by the complex sinusoidal plane wave. It can be defined as follows:

$$G(x, y) = \frac{f^2}{\pi\delta\eta} \exp\left(-\frac{x'^2 + \delta^2 y'^2}{2\sigma^2}\right) \exp(j2\pi fx' + \varphi) \quad (2)$$

$$x' = x \cos \theta + y \sin \theta \quad (3)$$

$$y' = -x \sin \theta + y \cos \theta \quad (4)$$

where θ represents the direction of the parallel strips in the Gabor filter kernel, and the effective value is a real number

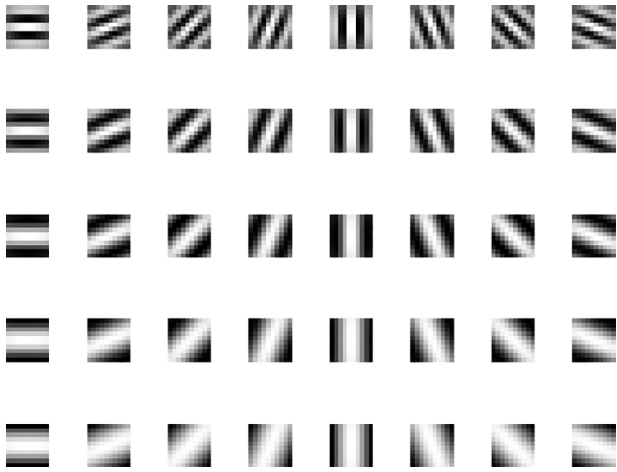


Figure 1. Gabor filter in 5 scales and 8 orientations.

from 0° to 360° ; φ is the phase offset of the cosine function, and the effective value ranges from -180° to 180° ; δ is the spatial aspect ratio; σ represents the standard deviation of the Gaussian function in the Gabor kernel function; and f is the frequency of the sinusoid.

In our work, we use 40 Gabor filters in 5 scales and 8 orientations, which are shown in Figure 1. After using 40 Gabor filters, because of the high correlation of feature vectors, we can reduce the reduced feature data by way of downsampling for reducing information redundancy.^{31,32} Therefore, the protein sequence can be represented as Gabor feature vectors that are constructed by the first 100 coefficients.

Random forrest classifier

At present, RF is one of the most popular prediction algorithms in data science. It was mainly developed by Breiman.²³ The RF model is one of the efficient ensemble classification algorithms, which uses multiple decision trees to reduce the output variance, thereby improving the accuracy of the classification. The RF classification makes full use of 2 powerful machine learning techniques. The first of RF classification is the selection of training examples, assuming that the original sample set has the total of examples $N = (((V_1, V_2, V_3, \dots, V_n), y), \dots)$, where V denotes the feature of each sample and y represents a class label; each round is extracted from the original sample set by bootstrap (with replacement sampling). It is worth noting that when drawing the training set of the current tree by replacing the samples, about 36.8% of the cases are omitted from the samples. We treat it as out-of-bag (OOB), which can be used to evaluate the performance of the decision tree and calculate the prediction error rate of the model called the OOB data error. The second is a select feature that in each classification tree mainly samples a small fraction of features at each node. Specifically, RF randomly selects a part of features from the complete features to form a new feature set and uses the new feature set to generate a decision tree when the Gini index reaches its maximum. Then, the data are divided into 2 subsets: positive and

negative. Loop the 2 steps to build the RF multiple times and finally use the voting mechanism to get the final classification result.

Results and Discussion

Evaluation measures

To better evaluate the proposed method, we calculated the following evaluation parameters: precision (PR), prediction accuracy (ACC), sensitivity (SN), specificity (SPC), and Matthew's correlation coefficient (MCC). Their formation can be seen as follows:

$$ACC = \frac{TP+TN}{TP+FP+TN+FN} \quad (5)$$

$$SN = \frac{TP}{TP+FN} \quad (6)$$

$$PR = \frac{TP}{TP+FP} \quad (7)$$

$$SPC = \frac{TN}{TN+FP} \quad (8)$$

$$MCC = \frac{TP \times TN - FP \times FN}{\sqrt{(TP+FP) \times (TN+FN) \times (TN+FP) \times (TP+FN)}} \quad (9)$$

where true negative (TN) is the number of true noninteracting pairs that are predicted correctly; true positive (TP) is the number of true samples that are predicted correctly; false positive (FP) is the number of true noninteracting pairs that are predicted to be interacting; and false negative (FN) is the correct number of samples that are predicted incorrectly. Moreover, the receiver operating characteristic (ROC) curves are one of the ways to evaluate the performance of the proposed method, and based on the prediction result, the area under an ROC curve (AUC) can also be computed to summarize ROC curve numerically.

Assessment of prediction ability

To ensure fairness of experiments, we conducted experiments in 3 different data sets of *yeast*, *human*, and *Helicobacter pylori*. We set the same corresponding parameters ($N-tree = 100$) in an RF classifier. Furthermore, to increase the credibility of our method, we adopted a 5-fold cross-validation to divide the whole data set into 5 parts, of which one-fifth is used for testing and four-fifths are used for training. By doing this, we can generate 5 models from the original data set. The prediction result based on RF classification models of protein sequence on 3 data sets is shown in Tables 1 to 3.

As shown in the tables, when predicting PPIs of *yeast* data set, the proposed approach can obtain prediction performance with an average accuracy, precision, sensitivity, specificity, and MCC of 92.10%, 93.85%, 90.09%, 94.10%, and 85.43% and standard deviations of 0.29%, 0.69%, 0.86%, 0.60%, and 0.49%,

Table 1. Five-fold cross-validation prediction results obtained on *yeast* data set.

TEST SET	ACC, %	PR, %	SN, %	SPC, %	MCC, %	AUC, %
1	92.18	92.87	90.91	93.38	85.56	95.85
2	91.60	93.88	88.78	94.35	84.57	95.34
3	92.31	94.47	90.38	94.37	85.80	95.24
4	92.13	93.50	90.68	93.60	85.50	96.02
5	92.27	94.53	89.70	94.82	85.71	96.13
Average	92.10 ± 0.29	93.85 ± 0.69	90.09 ± 0.86	94.10 ± 0.60	85.43 ± 0.49	95.72 ± 0.40

Abbreviations: ACC, accuracy; AUC, area under an ROC curve; MCC, Matthew's correlation coefficient; PR, precision; ROC, receiver operating characteristic; SN, sensitivity; SPC, specificity.

Table 2. Five-fold cross-validation prediction results obtained on *human* data set.

TEST SET	ACC, %	PR, %	SN, %	SPC, %	MCC, %	AUC, %
1	97.12	97.50	96.36	97.80	94.38	99.14
2	97.12	98.21	95.88	98.32	94.40	99.25
3	96.69	97.41	95.67	97.64	93.59	99.51
4	97.18	98.64	95.27	98.85	94.48	99.30
5	97.06	98.29	95.52	98.47	94.27	99.44
Average	97.03 ± 0.20	98.01 ± 0.53	95.74 ± 0.41	98.22 ± 0.50	94.22 ± 0.36	99.33 ± 0.15

Abbreviations: ACC, accuracy; AUC, area under an ROC curve; MCC, Matthew's correlation coefficient; PR, precision; ROC, receiver operating characteristic; SN, sensitivity; SPC, specificity.

Table 3. Five-fold cross-validation prediction results obtained on *Helicobacter pylori* data set.

TEST SET	ACC, %	PR, %	SN, %	SPC, %	MCC, %	AUC, %
1	86.11	88.13	83.62	88.62	76.05	92.56
2	85.08	87.89	83.01	87.36	74.58	91.74
3	87.14	89.29	84.75	89.58	77.56	91.01
4	87.31	87.73	85.87	88.67	77.80	92.00
5	86.62	89.49	81.85	91.06	76.64	92.15
Average	86.45 ± 0.90	88.51 ± 0.82	83.82 ± 1.55	89.06 ± 1.37	76.53 ± 1.30	91.89 ± 0.58

Abbreviations: ACC, accuracy; AUC, area under a ROC curve; MCC, Matthew's correlation coefficient; PR, precision; ROC, receiver operating characteristic; SN, sensitivity; SPC, specificity.

respectively. When predicting PPIs of *human* data set, the average accuracy, precision, sensitivity, specificity, and MCC are 97.03%, 98.01%, 95.74%, 98.22%, and 94.22% and standard deviations are 0.20%, 0.53%, 0.41%, 0.50%, and 0.36%, respectively. When predicting PPIs of *Helicobacter pylori* data set, the average accuracy, precision, sensitivity, specificity, and MCC are 86.45%, 88.51%, 83.82%, 89.06%, and 76.53% and standard deviations are 0.90%, 0.82%, 1.55%, 1.37%, and 1.30%, respectively. The ROC curves are shown in Figures 2 to 4. The y -ray depicts the true positive rate and the x -ray depicts the false

positive rate in these figures. Meanwhile, the AUC values were also computed and the results of *yeast*, *human*, and *Helicobacter pylori* data sets were 95.72%, 99.33%, and 91.89%, respectively.

According to these results, the method is both practical and effective for predicting PPIs by combining the Gabor feature with RF classification. Furthermore, these criterion values in low deviations indicate that the method we proposed is stable and robust. The main advantage of the feature extraction method is that it can not only retain enough prior information of PSSM but also describe the sequence information of protein

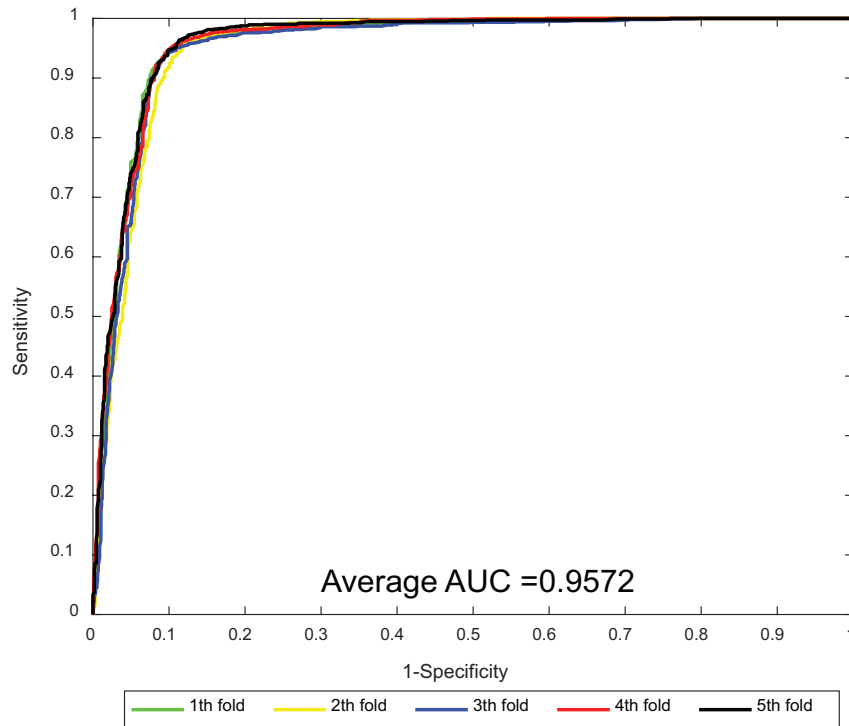


Figure 2. ROC curves performed by the proposed method on yeast protein-protein interaction data sets. AUC indicates area under an ROC curve; ROC, receiver operating characteristic.

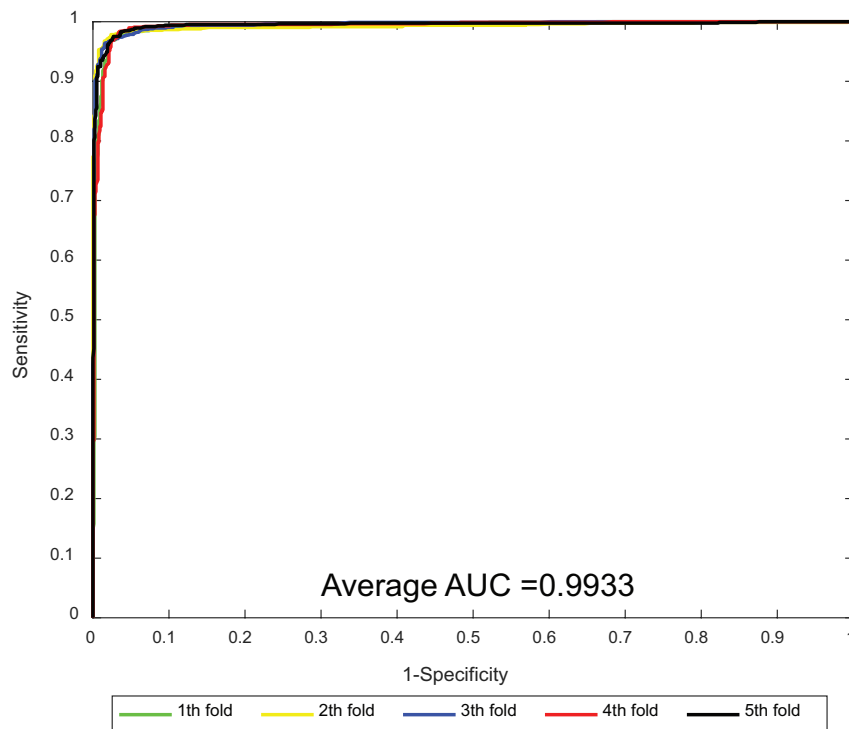


Figure 3. ROC curves performed by the proposed method on human protein-protein interaction data sets. AUC indicates area under an ROC curve; ROC, receiver operating characteristic.

sequence efficiently. The ability of the Gabor feature in obtaining effective information in PSSM is outstanding. Besides, considering the influence of protein sequence order, the texture information extracted by the Gabor feature can retain the

effective information of protein sequence well. The results show that the utilization of the Gabor texture feature to extract evolutionary information in predicting PPIs in the proposed method is effective.

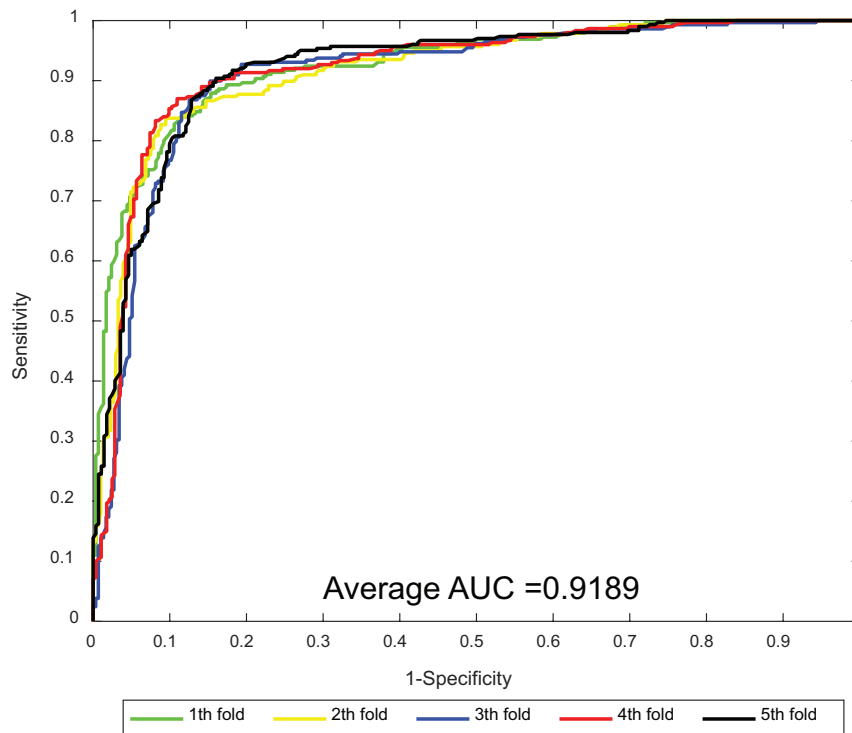


Figure 4. ROC curves performed by the proposed method on *Helicobacter pylori* protein-protein interaction data sets. AUC indicates area under an ROC curve; ROC, receiver operating characteristic.

Comparison with other feature extraction methods

To evaluate the effectiveness of the Gabor feature in extracting protein sequence information and identifying protein interactions, we further compared the results to DCT and LPQ with the same RF classification. The DCT algorithm is a popular linear separable transformation. It is mainly used for data or image compression, and DCT has a good performance of decorrelation due to its ability to convert signals from the spatial domain to the frequency domain. The LPQ is considered as an effective operator for texture feature descriptors, which remain the blur-invariant property, and the LPQ is also widely used in facial recognition and image processing. In our work, the DCT feature, the LPQ feature, and the Gabor feature were extracted from PSSM, and then we made a comparison in the same RF classification.

The results of *yeast* and *H. pylori* PPI data sets are presented in Figure 5. From Figure 5A to F, the Gabor feature basically dominates the LPQ feature and the DCT feature in terms of accuracy, specificity, sensitivity, precision, MCC, and AUC. In the *yeast* data set, the accuracy, specificity, and MCC gaps between Gabor and LPQ are 3.09%, 0.16%, and 4.45%, respectively. And the accuracy, specificity, and MCC gaps between Gabor and DCT are 0.50%, 0.23%, and 3.28%, respectively. Similarly, in the *Helicobacter pylori* data set, the accuracy, specificity, and MCC gaps between Gabor and LPQ are 6.22%, 4.35%, and 8.41%, respectively. And the accuracy, specificity, and MCC gaps between Gabor and DCT are 7.36%, 5.26%, and 9.73%, respectively. Thus, the Gabor

feature has little difference in specificity from LPQ and DCT, but, due to the difference in specificity from MCC, we speculate that the Gabor feature has better performance than LPQ in extracting texture feature of protein sequence, especially in enhancing the sequence information of a protein sequence. The Gabor feature is similar or even better than DCT in extracting protein sequence information.

Performance on the independent data sets

As we obtained good results on 3 PPI data sets of *yeast*, *human*, and *Helicobacter pylori*, for further evaluating the proposed method, we assumed that homologous proteins can preserve their ability to interact and used interactions experimentally identified in one organism to predict interactions in other organisms. The basis of this assumption is that homologs have similar functional behaviors. Therefore, they preserve the same PPI.³³ The 4 independent data sets we used share low identity with the training data set. Specifically, 11 188 samples from the *yeast* data set were used as the training data set. Then, we tested on 4 PPI data sets that were independent of the training data set. These data sets were treated as positive data sets that have been converted into PSSM. The experimental results of the 4 independent data sets are summarized in Table 4. The prediction performance accuracy was 93.20%, 94.89%, 91.93%, and 91.34% on *Caenorhabditis elegans*, *Mus musculus*, *Homo sapiens*, and *Helicobacter pylori*, respectively. It demonstrates that our proposed method can yield a superior prediction performance toward cross-species data sets.

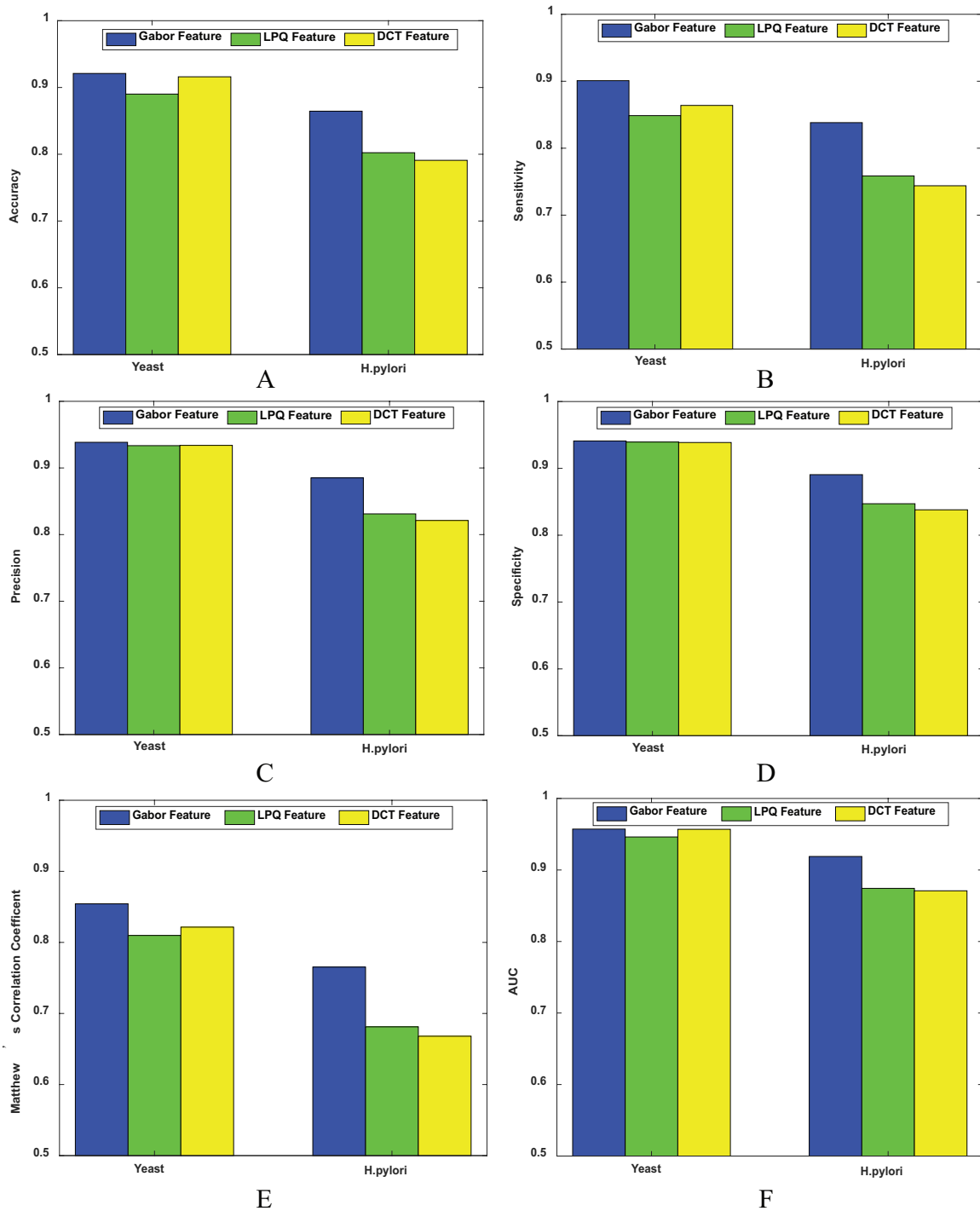


Figure 5. Performance comparison with 6 validation metrics using the Gabor feature (blue bar), the LPQ feature (green bar), and the DCT feature (yellow bar). (A) Accuracy rates, (B) sensitivity, (C) precision, (D) specificity, (E) MCC and (F) AUC. AUC indicates area under an ROC curve; DCT, discrete cosine transform; LPQ, local phase quantization; MCC, Matthew's correlation coefficient; ROC, receiver operating characteristic.

According to the results in Table 4, when the PPI data set from *yeast* was used as the positive samples to predict the PPIs of other cross-species, the prediction performance was effective. And it is noteworthy that the prediction model is constructed using *S. cerevisiae* PPI data set, so the trained model represented the characteristics of *S. cerevisiae* PPI. Meanwhile, a strong generalization ability demonstrates that the method we proposed is effective. Moreover, it is

reliable to assume that PPIs generated in one species can be used to predict PPIs in other species. The number of PPIs in one organism might have “coevolved” with another organism, so their corresponding orthologs interact as well.³⁴ This notion of conserved interactions is also supported by the observation that many interactions are conserved between different species in molecular machines or signal transduction pathways.³⁵

Table 4. Model prediction results of 4 species.

SPECIES	TEST PAIRS	ACC, %
<i>Caenorhabditis elegans</i>	4013	93.20
<i>Mus musculus</i>	313	94.89
<i>Homo sapiens</i>	1412	91.93
<i>Helicobacter pylori</i>	1420	91.34

Abbreviation: ACC, accuracy.

Table 5. Performance comparison of different methods on the *Helicobacter pylori* data set.

MODEL	ACC, %	PR, %	SN, %	MCC, %
Signature products ²⁹	83.40	85.70	79.90	N/A
Boosting ³⁶	79.52	81.69	80.37	70.64
Ensemble ELM ³⁷	87.50	86.15	88.95	78.13
Phylogenetic bootstrap ³⁸	75.80	80.20	69.80	N/A
Ensemble of HKNN ³⁹	86.60	85.00	86.70	N/A
HKNN ⁴⁰	84.00	84.00	86.00	N/A
Proposed method	86.45	88.51	83.82	76.53

Abbreviations: ACC, accuracy; ELM, extreme learning machine; HKNN, *K*-local hyperplane distance neighbor; MCC, Matthew's correlation coefficient; PR, precision; SN, sensitivity.

Comparison with other methods

In recent years, a large number of algorithms have emerged for predicting PPIs. In Table 5, we compared previous studies that proposed other methods to predict PPIs of *Helicobacter pylori* data set. The accuracy of other methods is between 75.80% and 87.50%; our proposed method is slightly lower than ensemble ELM (extreme learning machine) in accuracy, sensitivity, and MCC, so we assumed that ensemble ELM classification is more effective than RF classification in learning classification. We then compared our method with the existing methods of *yeast* and *human* data sets. The results of 6 other methods with accuracy ranging from 75.08% to 92.10% are shown in Table 6. The proposed method gets high average accuracy (92.10%), which is higher than other methods. The lower standard deviation also means that the performance of the proposed method is more robust. From Table 7, we can observe that the performance of our method is higher than that of previous work based on RF classification.

From the table above, we can see that using an ensemble classifier such as the ensemble of HKNN (*K*-local hyperplane distance nearest neighbor) and boosting is better than using a single classifier, which can achieve more accurate and robust performance. Through these comparisons, and compared with the most advanced methods at present, we can observe that the RF-based model combined with PSSM can improve the prediction accuracy directly. Feature extraction containing evolutionary information and the selection of classifiers are

the primary way to promotion. Meanwhile, its excellent performance demonstrates that the Gabor feature has a strong ability in extracting protein sequence information, especially enhancing protein texture features. Thus, effective feature extraction improves the performance of classification.

Conclusions and Discussion

In recent years, the number of researchers requiring more knowledge to detect PPIs is increasing. Due to the complexity and high dimensionality of proteomic data, flexible and powerful statistical learning tools are needed for effective statistical analysis, which promotes the rapid development of computing methods for predicting PPIs. In this article, we proposed a novel computational method for predicting PPIs in which an RF classifier combined with the Gabor feature descriptor on the PSSM is used. The main improvements of the proposed method are that the Gabor feature can extract the discriminative information of protein sequence, especially enhancing the texture feature information of protein sequence that the interaction between proteins is more likely to occur in the region with higher energy. The experimental results demonstrated that the good performance of our proposed method in predicting PPIs. The results also showed that Gabor features perform better than LPQ and DCT in texture feature and protein sequence correlation extraction. In future studies, more effective feature extraction methods and machine learning techniques will be explored for PPI prediction.

Table 6. Performance comparison of different methods on the yeast data set.

MODEL	TEST SET	ACC, %	PR, %	SN, %	MCC, %
Work by Yang et al ⁴¹	Cod1	75.08 ± 1.13	74.75 ± 1.23	75.81 ± 1.20	N/A
	Cod2	80.04 ± 1.06	82.17 ± 1.35	76.77 ± 0.69	N/A
	Cod3	80.41 ± 0.47	81.86 ± 0.99	78.14 ± 0.90	N/A
	Cod4	86.15 ± 1.17	90.24 ± 1.34	81.03 ± 1.74	N/A
Work by You et al ³⁷	PCA-EELM	87.00 ± 0.29	87.59 ± 0.32	86.15 ± 0.43	77.36 ± 0.44
Work by Guo et al ⁴²	AC	87.36 ± 1.38	87.82 ± 4.33	87.30 ± 4.68	N/A
	ACC	89.33 ± 2.67	88.87 ± 6.16	89.93 ± 3.68	N/A
Work by Zhou et al ⁴³	SVM + LD	88.56 ± 0.33	89.50 ± 0.60	87.37 ± 0.22	77.15 ± 0.68
Proposed method	RF	92.10 ± 0.29	93.85 ± 0.69	90.09 ± 0.86	85.43 ± 0.49

Abbreviations: ACC, accuracy; LD, local descriptor; MCC, Matthew's correlation coefficient; PCA-EELM, principal component analysis-ensemble extreme learning machine; PR, precision; RF, random forest; SN, sensitivity; SVM, support vector machine.

Table 7. Performance comparison of different methods on the human data set.

MODEL	ACC, %	PR, %	SN, %	MCC, %
AC + SVM ⁴⁴	89.3	N/A	94.0	79.2
AC + RF ⁴⁴	95.5	N/A	94.0	91.4
AC + RoF ⁴⁴	95.1	N/A	93.3	91.0
LDA + SVM ⁴⁴	90.7	N/A	89.7	81.3
LDA + RoF ⁴⁴	95.7	N/A	97.6	91.8
LDA + RF ⁴⁴	96.4	N/A	94.2	92.8
Proposed method	97.03	98.01	95.74	94.22

Abbreviations: ACC, accuracy; LDA, latent Dirichlet allocation; MCC, Matthew's correlation coefficient; PR, precision; RF, random forest; RoF, rotation forest; SN, sensitivity; SVM, support vector machine.

Author Contributions

XKZ and ZHY conceived and designed the analysis. ZHY and LPL provided data. YL, ZW and XZK provided mathematical theory and performed simulations. XZK and JP wrote the manuscript. All authors reviewed the final manuscript.

REFERENCES

- Ho Y, Gruhler A, Heilbut A, et al. Systematic identification of protein complexes in *Saccharomyces cerevisiae* by mass spectrometry. *Nature*. 2002;415:180-183.
- Zhu H, Snyder M. Protein chip technology. *Curr Opin Chem Biol*. 2003;7:55-63.
- Brückner A, Polge C, Lentze N, et al. Yeast two-hybrid, a powerful tool for systems biology. *Int J Mol Sci*. 2009;10:2763-2788.
- Vidalain P-O, Boxem M, Ge H, Li S, Vidal M. Increasing specificity in high-throughput yeast two-hybrid experiments. *Methods*. 2004;32:363-370.
- You Z-H, Lei Y-K, Gui J, Huang DS, Zhou X. Using manifold embedding for assessing and predicting protein interactions from high-throughput experimental data. *Bioinformatics*. 2010;26:2744-2751.
- Joshi T, Chen Y, Becker JM, Alexandrov N, Xu D. Genome-scale gene function prediction using multiple sources of high-throughput data in yeast *Saccharomyces cerevisiae*. *OMICS*. 2004;8:322-333.
- Qi Y, Klein-Seetharaman J, Bar-Joseph Z. Random forest similarity for protein-protein interaction prediction from multiple sources. In: Altman RB, Jung TA, Klein TE, Dunker AK, Hunter L, eds. *Bioinformatics 2005*. Singapore: World Scientific; 2005:531-542.
- Peri S, Navarro JD, Kristiansen TZ, et al. Human protein reference database as a discovery resource for proteomics. *Nucleic Acids Res*. 2004;32:D497-D501.
- Salwinski L, Miller CS, Smith AJ, Pettit FK, Bowie JU, Eisenberg D. The database of interacting proteins: 2004 update. *Nucleic Acids Res*. 2004;32:D449-D451.
- Licata L, Briganti L, Peluso D, et al. MINT, the molecular interaction database: 2012 update. *Nucleic Acids Res*. 2011;40:D857-D861.
- Biasini M, Bienert S, Waterhouse A, et al. SWISS-MODEL: modelling protein tertiary and quaternary structure using evolutionary information. *Nucleic Acids Res*. 2014;42:W252-W258.
- Peng J, Xu J. RaptorX: exploiting structure information for protein alignment by statistical inference. *Proteins*. 2011;79:161-171.
- Yu H-J, Huang D-S. Graphical representation for DNA sequences via joint diagonalization of matrix pencil. *IEEE J Biomed Health Inform*. 2013;17:503-511.
- Nishikawa K, Noguchi T. [3] Predicting protein secondary structure based on amino acid sequence. In: Langone JJ, ed. *Methods in Enzymology*. Vol. 202. Amsterdam, The Netherlands: Elsevier; 1991:31-44.
- Feng P-M, Lin H, Chen W. Identification of antioxidants from sequence information using naive Bayes. *Comput Math Methods Med*. 2013;2013:567529.
- Gill SC, Von Hippel PH. Calculation of protein extinction coefficients from amino acid sequence data. *Anal Biochem*. 1989;182:319-326.

17. Mohabatkar H, Beigi MM, Abdolahi K, Mohsenzadeh S. Prediction of allergenic proteins by means of the concept of Chou's pseudo amino acid composition and a machine learning approach. *Med Chem*. 2013;9:133-137.
18. Liu B, Wang X, Zou Q, Dong Q, Chen Q. Protein remote homology detection by combining Chou's pseudo amino acid composition and profile-based protein representation. *Mol Inform*. 2013;32:775-782.
19. Zou H-L, Xiao X. Classifying multifunctional enzymes by incorporating three different models into Chou's general pseudo amino acid composition. *J Membr Biol*. 2016;249:551-557.
20. Jaakkola TS, Diekhans M, Haussler D. Using the Fisher kernel method to detect remote protein homologies. *Proc Int Conf Intell Syst Mol Biol*. 1999;99:149-158.
21. Shen J, Zhang J, Luo X, et al. Predicting protein-protein interactions based only on sequences information. *Proc Natl Acad Sci USA*. 2007;104:4337-4341.
22. Leslie C, Eskin E, Cohen A, Weston J, Noble WS. Mismatch string kernels for discriminative protein classification. *Bioinformatics*. 2003;20:467-476.
23. Breiman LJ. Random forests. *Mach Learn*. 2001;45:5-32.
24. Jones DT. Protein secondary structure prediction based on position-specific scoring matrices. *J Mol Biol*. 1999;292:195-202.
25. Jeong JC, Lin X, Chen X-W. On position-specific scoring matrix for protein function prediction. *IEEE/ACM Trans Comput Biol Bioinform*. 2010;8:308-315.
26. Ahmed N, Natarajan T, Rao KR. Discrete cosine transform. *IEEE Trans Comput*. 1974;100:90-93.
27. Ojansivu V, Heikkilä J. Blur insensitive texture classification using local phase quantization. Paper presented at: International Conference on Image and Signal Processing; July 1-3, 2008:236-243; Cherbourg-Octeville, France. https://link.springer.com/chapter/10.1007/978-3-540-69905-7_27.
28. You Z-H, Yu J-Z, Zhu L, Li S, Wen ZK. A MapReduce based parallel SVM for large-scale predicting protein-protein interactions. *Neurocomputing*. 2014;145:37-43.
29. Martin S, Roe D, Faulon J-L. Predicting protein-protein interactions using signature products. *Bioinformatics*. 2004;21:218-226.
30. Gabor D. Theory of communication. Part 1: the analysis of information. *J Inst Electr Eng III: Radio Commun Eng*. 1946;93:429-441.
31. Yang M, Zhang L, Shiu SC, et al. Gabor feature based robust representation and classification for face recognition with Gabor occlusion dictionary. *Pattern Recogn*. 2013;46:1865-1878.
32. Shen L, Bai L. Gabor feature based face recognition using kernel methods. Paper presented at: Sixth IEEE International Conference on Automatic Face and Gesture Recognition; May 19, 2004:170-176; Seoul, South Korea. <https://ieeexplore.ieee.org/abstract/document/1301526/references#references>.
33. Shi M-G, Xia J-F, Li X-L, Huang DS. Predicting protein-protein interactions from sequence using correlation coefficient and high-quality interaction dataset. *Amino Acids*. 2010;38:891-899.
34. Smialowski P, Pagel P, Wong P, et al. The Negatome database: a reference set of non-interacting protein pairs. *Nucleic Acids Res*. 2010;38:D540-D544.
35. Matthews LR, Vaglio P, Reboul J, et al. Identification of potential interaction networks using sequence-based searches for conserved protein-protein interactions or "interologs." *Genome Res*. 2001;11:2120-2126.
36. Liu B, Yi J, Sv A, et al. QChIPat: a quantitative method to identify distinct binding patterns for two biological ChIP-seq samples in different experimental conditions. *BMC Genomics*. 2013;14:S3.
37. You Z-H, Lei Y-K, Zhu L, Xia J, Wang B. Prediction of protein-protein interactions from amino acid sequences with ensemble extreme learning machines and principal component analysis. *BMC Bioinformatics*. 2013;14:S10.
38. Bock JR, Gough DA. Whole-proteome interaction mining. *Bioinformatics*. 2003;19:125-134.
39. Nanni L, Lumini A. An ensemble of K-local hyperplanes for predicting protein-protein interactions. *Bioinformatics*. 2006;22:1207-1210.
40. Nanni L. Hyperplanes for predicting protein-protein interactions. *Neurocomputing*. 2005;69:257-263.
41. Yang L, Xia J-F, Gui J. Prediction of protein-protein interactions from protein sequence using local descriptors. *Protein Pept Lett*. 2010;17:1085-1090.
42. Guo Y, Yu L, Wen Z, Li M. Using support vector machine combined with auto covariance to predict protein-protein interactions from protein sequences. *Nucleic Acids Res*. 2008;36:3025-3030.
43. Zhou YZ, Gao Y, Zheng YY. Prediction of protein-protein interactions using local description of amino acid sequence. In: Zhou M, Tan H, eds. *Advances in Computer Science and Education Applications*. Berlin, Germany: Springer; 2011:254-262.
44. Liu B, Liu F, Fang L, Wang X, Chou KC. repDNA: a Python package to generate various modes of feature vectors for DNA sequences by incorporating user-defined physicochemical properties and sequence-order effects. *Bioinformatics*. 2014;31:1307-1309.